Explosion disaster distribution characteristics and outlet open-close effect of turning roadway

Pengfei Lv
Beijing Institute of Petrochemical Technology
Minghua Ju
Beijing Institute of Petrochemical Technology
Jiaxu Zhang
Beijing Institute of Petrochemical Technology
Lei Pang (pang@bipt.edu.cn)
Beijing Institute of Petrochemical Technology
Kai Yang
Beijing Institute of Petrochemical Technology

Research

Keywords: explosion shock waves, turning roadway, disaster distribution, open-close effect

DOI: https://doi.org/10.21203/rs.3.rs-59697/v1

Abstract

In this study, under the open-close conditions of a roadway outlet, the nonlinear dynamic analysis finite element program ANSYS/LS-DYNA was used to build models of explosions on roadways with 0˚ and 90˚ bending angles, to compare and analyse the shock wave propagation characteristics and variation laws. Moreover, the destructive effect of the explosion on the partition was analysed based on the level of damage caused to the human body by shock wave overpressure. The results show that the bending angle has an impact on the space-time distribution law of the explosion shock waves on the roadway. As the bending angle increases, the peak overpressure attenuation of the shock waves becomes prominent, and the arrival time for the same distance increases. The closure of the roadway outlet has a distance effect on the peak overpressure of the shock waves. The explosion shock waves cause the peak overpressure to rise sharply owing to the reflection and stacking effects near the closure. In the far zone of the outlet, the attenuation of the shock waves is too fast and has minimal impact on the peak overpressure. Additionally, overall, the closure of the roadway outlet increases the damage range of the explosion shock waves and the severity of their effect on the human body. With an increase in the bending angle, the damage range and severity decrease. These results can provide a reference for explosion disaster evaluation and prevention.

1. Introduction

An underground roadway is a typical underground confined space where the characteristics of dynamite explosions differ greatly from those in an open space. Once an accidental explosion occurs in the roadway, the shock waves cannot quickly propagate due to the confined space, thus increasing the overpressure duration and creating enormous threats for personnel and equipment. Worse still, any barrier in the roadway, or the closure of the outlet, could further intensify the reflection process and the damaging effects. The research on explosion shock waves in roadways is important not only for the evaluation of combat measures effectiveness, but also as a foundation for the analysis of accidental explosion system safety. Turning structures have been widely used in industrial, civil, and military roadway facilities; therefore, it is extremely necessary to study the distribution characteristics of explosion disasters, as well as the safety protection.

The most effective way to study the explosion shock waves process is to carry out explosive experiments. Dadone et al. (1971) performed five types of tunnel experiments to study the pressure attenuation of shock waves passing through interaction points. The results showed that the pressure attenuation of shock waves at the interaction points could neglect the tunnel size effect. The calculation of the shock wave pressure changes near the interaction points, based on the steady flow pressure model, presented large errors. Savenk (1979) studied the propagation characteristics and shock waves laws based on a model experiment. The attenuation coefficients of the shock waves were obtained through the local variation in bifurcation and turning. Limited by the research conditions, he was unable to perform in-depth research in this field. Smith et al. (1992) obtained the explosive point's overpressure time and propagation characteristics through explosion experiments in tunnels with different coarseness levels

and loads. Britan et al. (2001; 2006) analysed the effect of spheroidal particle filter parameters on shock wave attenuation. Based on the study of the change laws of shock waves passing through porous mediums with different geometric shapes and porosity, they proposed basic ideas of optimum underground space structural design. Pang et al. (2013) conducted explosive experiments in tunnels with various turning angles and obtained the distribution law of a high-temperature flow field before and after the turning.

Given the complexity of the explosion effects and difficult operation conditions, with the development of computer technology, numerical simulations can be used to study the explosive process. Given their low computational cost and wide range of data, numerical simulations have already been widely used (Chan et al., 1994; Janovsky et al., 2006; Benselama et al., 2010; Wang et al., 2012; Sugiyama et al., 2014; Wang et al., 2016). Using simulations, Igra et al. (1998) studied the shock waves' propagation characteristics in a 90˚ branch pipe. The complicated, unsteady flow formed was affected by the shock waves and branch pipes. Rigas and Sklavounos (2005) adopted computational fluid dynamics to analyse the shock waves' propagation in tunnels with complex geometrical shapes. The results indicated that the incident overpressure was far greater than the propagation overpressure. Luccioni et al. (2006) put forward a grid size for explosive analysis, improving the precision of analyses. Ohtomo et al. (2005) studied the propagation laws of shock waves passing through shock tunnels filled with inclined and staggered boards. The results showed that a shock wave attenuation occurred, and the effect was more obvious in shock tunnels filled with inclined boards. Berger et al. (2010) investigated the impact of a single group of barriers and multiple groups of barriers on shock wave propagation characteristics in shock tunnels. The results revealed that the geometrical shapes of the barriers play a key role in the shock wave attenuation, with a big blocking ratio. Zhao et al. (2012) analysed the structure strength and damage effect of a coal mine mobile refuge chamber under an explosion load. Zhang et al. (2010; 2013) used numerical simulation to study the explosion shock waves' peak pressure distribution when passing a 20˚, 45˚, 90˚, and 135˚ one-way turning roadway, and revealed the influences of roadway geometry on the shock wave propagation laws. Additionally, the shock wave propagation laws in 45˚, 90˚, 135˚, Y-shape, and T-shape branched roadways were also simulated and studied.

The results of previous studies show that investigations of explosion shock wave propagation laws have mainly focused on straight roadways. Although some researchers have considered the impacts of bending angles and geometry, there are fewer studies on the shock wave propagation characteristics in continuous turning roadways. Furthermore, the open-close conditions of a roadway outlet's influence on shock wave propagation characteristics, and its destructive effect, are less researched. This paper builds, through numerical simulation, and based on the roadway outlet's open-close conditions, respectively, models to analyse explosions in a roadway with 0˚ and 90˚ bending angles. The effect of the roadway outlet conditions on the shock wave propagation characteristics is analysed. Additionally, the explosive destruction effect partition is analysed based on the level of damage caused to the human body by the shock wave overpressure.

2. Numerical Simulation

2.1. Explosion analysis model

A nonlinear dynamic analysis finite element program called ANSYS/LS-DYNA is used to conduct a numerical simulation to study the open-close conditions of the influence of different turning roadway outlets on the explosion shock wave propagation characteristics. The bending angle between tangent line OA and straight line OB is marked as θ, as shown in Fig. 1(a). According to the value of θ, two roadways with different curvatures are built, as shown in Fig. 1(b). The bending angles are 0˚ and 90˚, respectively.

The simulated sectional dimension of the roadway is 3.5 m × 3.5 m, and the explosive source is located in the section core. The roadway with θ = 0° is taken as an example. Half of the three-dimensional explosion analysis models have been built according to symmetry, as seen in Fig. 2. Figure 2(a) is the model with the roadway outlet closure, that is, the roadway outlet is under a barrier sealing treatment. Figure 2(b) is the model with the open roadway outlet. The horizontal length of the roadway is 100 m, and the distance between the roadway outlet and the explosive source is also 100 m.

To facilitate the analysis, the explosive source is taken as the origin of the coordinate system. Roadways with different curvatures are projected on the roadway with θ = 0°. The vertical distance between the projection line and the explosive source is taken as the spacing, and the intersection of each projection line and the different curvature roadways are taken as survey points. Taking 10 m of spacing as an example, the roadway points with different curvatures are obtained, as shown in Fig. 3.

2.2. Material constitutive and state equation

The numerical simulation analysis of the explosive issues plays an important role in the study of the explosion mechanics. As an effective tool for nonlinear impact dynamics analysis, the ANSYS/LS-DYNA software can effectively simulate the explosive process in various mediums, as well as different engineering blasting issues. The Lagrange and Euler algorithms are commonly used in numerical simulations. Among them, the Lagrange algorithm is often used to analyse problems involving solid mechanics, while the Euler algorithm is used more for fluid mechanics analysis. The explosion in different turning roadways is the interaction between the detonation gas and the solid walls, which is a typical fluid-structure interaction. Therefore, the ALE algorithm is adopted to solve the problem of large deformation calculations, combining the advantages of the Lagrange and Euler algorithms.

For an easier analysis, the explosive source is 5 Kg TNT with a 1640 kg/m^3 charge density and 6930 m/s explosive velocity. The explosive adopts the MAT_HIGH_EXPLOSIVE_BURN constitutive model provided by LS-DYNA. Given that the explosive gas exhibits substantial pressure fluctuations in the numerical simulation, ranging from hundreds of thousands of atmospheres to lower than one atmosphere, it is difficult to find the appropriate state equation of the explosion pressure variation range. JWL's (LSTC, 2003) state equation is used in LS-DYNA to describe the relationship between the pressure and the volume variation of the detonation products. In JWL's state equation, the P-V relationship is as follows:

$$P = A\left(1-\frac{\omega}{R_1V}\right)e^{-R_1V} + B\left(1-\frac{\omega}{R_2V}\right)e^{-R_2V} + \frac{\omega E_0}{V} \quad (1)$$

where P refers to the pressure, and V refers to the volume. E_0 is the internal energy initial density. A, B, R_1, R_2, and ω are constants with values of 3.74, 0.0743, 4.1500001, 0.95, and 0.3, respectively.

The air adopts the MAT_NULL material model provided by LS-DYNA. Its state equation can be expressed as follows:

$$P = C_0 + C_1\mu + C_2\mu^2 + C_3\mu^3 + (C_4 + C_5\mu + C_6\mu^2)E \quad (2)$$

where P is the instantaneous pressure, $\mu = \rho/\rho_0 - 1$, and ρ/ρ_0 is the ratio between the instantaneous density ρ and the initial density ρ_0. The value of ρ_0 is 1.29 kg/m^3. E refers to the internal energy of a volume unit. C_0–C_6 are constants with values of 0, 0, 0, 0, 0.4, 0.4, and 0, respectively.

The mechanical properties of the roadway wall affect the explosion shock waves. In real roadways, the materials are mainly solid rocks or concrete, whose intensities are far greater than the intensity of the shock waves obtained by numerical simulation. Therefore, the roadway walls can be viewed as rigid materials, and their structural damage and elastic deformation effects on the shock wave reflection and stacking process can be neglected.

3. Results And Discussion

3.1. Results validation

The roadway with $\theta = 0°$ and open outlet is taken as an example to verify the reliability of the numerical simulation results. The shock wave peak overpressure in the unit of different positions is chosen as the study object. Subsequently, the shock wave overpressure and time changing curve are obtained, and the numerical simulation result is compared with the result obtained by Qin (2008), as shown in Fig. 4.

Figure 4 indicates that the numerical simulation result is consistent with the shock wave-overpressure/time-variation trend. Initially, the curve decreases sharply from the maximum, and then changes slowly, and becomes stable. The maximum survey point error is 17 KPa, and the average error is 6 KPa. The two curves are very close, indicating the higher reliability and feasibility of the numerical simulation results presented herein.

3.2. The effect of roadway outlet conditions on distribution of shock wave peak overpressure

In order to study the conditions of the roadway outlet's effect on the explosion shock waves, the air shock wave overpressures in different positions in the roadways with 0˚ and 90˚ blending angles are selected, to obtain the peak overpressure-distance distribution, as shown in Fig. 5.

As seen in Fig. 5, when θ = 0°, the shock wave peak overpressure is essentially equal in the region of 0–80 m from the explosive source under the condition of roadway outet closure and open. The roadway outlet closure has negligible impact on the shock wave peak overpressure. When the distance to the explosive source is 80–100 m and the roadway outlet is closed, the shock wave peak overpressure suddenly rises, showing an upward trend. In contrast, the shock wave peak overpressure decreases gradually when the roadway outlet is open. When θ = 90°, the peak overpressure distribution has similar features, but differs in different regions, i.e., when the distance to the explosive source is between 0 m and 90 m, the shock wave peak overpressure is essentially equal the same the condition of roadway outlet closure and open. When the distance is between 90 m and 100 m, the shock wave peak overpressure increases under the condition of roadway outlet closure, and reduces with the outlet open.

To further study the effect of the roadway outlet conditions on the explosion shock wave overpressure distribution in different turning roadways and regions, when θ = 0°, the roadway is divided into two zones by an 80 m distance to the explosive source as the boundary; that is, one zone is between 10 m and 70 m, and the other zone is between 80 m and 100 m. When θ = 90°, the roadway is divided into two zones by a 90 m distance to explosive source as the boundary; that is, a 10–80 m zone, and a 90–100 m zone. Subsequently, the corresponding explosion shock wave overpressure and time distribution curves are obtained, under the condition of roadway outlet closure and open, as shown in Figs. 6 and 7.

As seen in Figs. 6(a), 6(b), 7(a), and 7(b), the time changing curves of the shock wave overpressure in different positions are similar to the roadway outlet closure ones. Initially, the peak pressure increases from zero to the maximum, then decreases continuously, increases again to peak, and then begins to reduce. There are two peak values except at the outlet position. One is formed by shock waves passing through different positions after the explosion. The other is formed when the shock waves pass the barriers at the outlet, where only one peak is formed after the stacking of two peaks, and the peak pressure is considerably greater than the second peak pressure in other observation points. Furthermore, the comparison between Figs. 6(a) and 7(a), and 6(b) and 7(b) indicates that the peak pressure when θ = 90˚ decreases and the arrival time to the same distance increases, compared with those when θ = 0˚. Under the condition of outlet closure, two peak overpressures are chosen to obtain their distribution curves in different turning roadways, as seen in Fig. 8.

In the Figs. 8(a) and 8(b), the first peak overpressure overall decreases (excluding at the outlet points) with the increase in the propagation distance, while the second peak overpressure shows opposite characteristics, with the peak overpressure rising gradually as the propagation distance increases, especially at the outlet, where the peak overpressure reaches its maximum. These analyses suggest that, when the outlet is closed, the explosion shock waves have little effect on peak overpressure in the far zone of outlet, due to the shock waves decreasing greatly after the barriers' reflection away from the outlet. While the explosion shock waves reflection and stacking effects cause peak overpressure increase in the outlet near zone, the maximum peak pressure is formed in the curve. It can be seen that the closed condition of the roadway has a distance effect on the shock wave peak overpressure in the roadway.

Based on Figs. 6(c) and 6(d), 7(c) and 7(d), when the roadway outlet is open, the variation curves of the shock wave overpressure in different positions will increase from zero to peak, and then begin to reduce sharply. In contrast, when the roadway is closed, the pressure curves peak is formed only once. Moreover, the shock wave peak overpressure decreases with the propagation distance increase. Furthermore, the comparison between Figs. 6(c) and 7(c), 6(d) and 7(d) indicates that, as the θ bending angle of the roadway increases, the peak overpressure at the same distance decreases continuously, and the arrival time to the same distance increases. Therefore, the bending angle can change the space-time distribution of the shock wave overpressure in the roadway.

3.3. The influence of roadway outlet conditions on explosive destructive effect partition

Based on the explosion shock wave overpressure's level of injury to the human body shown in Table 1 (Gu et al., 2009), when the shock wave overpressure is more than 100 KPa in the explosion-affected zone, the zone will be regarded as the dead zone (marked by Zone A). When the shock wave overpressure is between 50 KPa and 100 KPa, the zone will be considered as a serious damage zone (marked by Zone B). When the shock wave overpressure is between 30 KPa and 50 KPa, the zone is identified as a moderate damage zone (marked by Zone C). When the shock wave overpressure is between 20 KPa and 30 KPa, the zone is determined as a slight damage zone (marked by Zone D). When the shock wave overpressure is between 0 KPa and 20 KPa, the zone is determined as a no damage zone (marked by Zone E). Combined with the numerical simulation results, Figs. 9 and 10 show the explosive destruction effect partition in the roadways with 0˚ and 90˚ bending angles, under the condition of roadway outlet closure and open. Table 2 shows each zone range for different curvature turning roadways, based on the explosive destruction effect partition.

Table 1
Explosion shock wave overpressure' level of injury to human body

Overpressure (KPa)	injury effect
< 20	no injuries but be scared
20 ~ 30	minor injury
30 ~ 50	hearing organ injury or fracture
50 ~ 100	severe visceral injury or death
> 100	the majority of deaths

Table 2
Range of explosive destruction effect partition of different curvature turning roadway

roadway type		explosion damage range/m				
		zone A	zone B	zone C	zone D	zone E
$\theta = 0^{\circ}$	with outlet closure	(0, 8.64)	(8.64, 18.94)	(18.94, 44.7), (93.18, 100)	(44.7, 93.18)	—
	with outlet open	(0, 8.44)	(8.44, 18.8)	(18.8, 47.37)	(47.37, 96.24)	(96.24, 100)
$\theta = 90^{\circ}$	with outlet closure	(0, 0.5)	(0.5, 2.87)	(2.87, 16.54), (99.46, 100)	(16.54, 65), (95.96, 99.46)	(65, 95.96)
	with outlet open	(0, 0.55)	(0.55, 2.96)	(2.96, 16.44)	(16.44, 65.33)	(65.33, 100)

In Fig. 9 and Table 2, when the outlet of the roadway with 0˚ bending angle is closed, zones A, B, C, and D are formed in the roadway after the explosion. When the roadway outlet is open, zones A, B, C, D, and E are formed. Comparing between the range of zones when the roadway outlet is closed and open, the ranges of zones A (dead zone) and B (serious damage zone) are essentially the same. When the roadway outlet is closed, the zone C (moderate damage zone) range increases visibly, and causes the zone D (slight damage zone) range to move forward.

In Fig. 10 and Table 2, when the outlet of the roadway with a 90˚ bending angle is closed, zones A, B, C, D, and E are formed in the roadway after explosion. Comparing between the range of zones with the open and closed outlet, the ranges of zones A (dead zone) and zone B (serious damage zone) are essentially equal. However, when the outlet is closed, the zone C (moderate damage zone) and zone D (slight damage zone) ranges increase visibly, and the zone E (no damage zone) range decreases.

Overall, the closure of the roadway outlet increases the damage range of the explosion shock waves and the severity of their impact on the human body. In addition, when the roadway outlet is closed and the bending angle of the roadway is 0˚, the ranges from A to C are clearly larger than the corresponding ranges when the bending angle is 90˚. The zone D (slight damage zone) and zone E (no damage zone) ranges decrease visibly, indicating that the damage range and severity decreases with the increase in the roadway bending angle.

4. Conclusions

(1) The bending angle can change the space-time distribution of the explosion shock waves in the roadway. As the roadway bending angle increases, the shock wave peak overpressure attenuation is obvious, and the arrival time to the same distance is increasing. When the roadway outlet is closed, the explosion shock waves will cause the peak overpressure to rise sharply after the reflection and stacking effects in the near zone of the outlet. In the far zone of the outlet, the shock wave effects on peak

overpressure is lighter due to the rapid attenuation after reflection. Therefore, the closure of the roadway outlet has a distance effect on the shock wave peak overpressure.

(2) According to the level of injury to the human body caused by the explosion shock wave overpressure, the explosion-affected zones in the roadway can be classified into dead zones, serious-damage zones, moderate-damage zones, slight-damage zones, and no-damage zones. The increase in the bending angle can, overall, reduce the explosive damage range and severity. However, the closure of the roadway outlet can, overall, increase the explosive damage range and severity. It can be seen that the bending angle and outlet conditions affect the distribution characteristics of the explosion disaster in the turning roadway. This research can provide a reference for explosion disaster evaluation and accident analysis in roadways.

Declarations

Acknowledgments

The authors thank the financial support of the National Nature Science Foundation of China (Grant No. 51604031), the Supporting Plan for the Construction of High-level Teachers in Beijing Universities in 2019 (Grant No. CIT&TCD201904045), the Key Technology Project of Safety Production in 2017 of China (Grant No. beijing-0007-2017AQ), and the Beijing Natural Science Foundation Municipal Education Committee Joint Funding Project (Grant No. KZ201910017020). Meanwhile, we thank English translation service provided by Beijing T-norm Translation Service Co., Ltd, and thank Elsevier for retouching the language.

References

1. Benselama AM, William-Louis MJP, Monnoyer F, Proust C (2010) A numerical study of the evolution of the blast wave shape in tunnels. J Hazard Mater 183(1–3):609–616
2. Berger S, Sadot O, Ben-Dor G (2010) Experimental investigation on the shock-wave load attenuation by geometrical means. Shock Waves 20(1):29–40
3. Britan A, Ben-Dor G, Igra O, Shapiro H (2001) Shock waves attenuation by granular filters. Int J Multi Flow 27(4):617–634
4. Britan A, Igra O, Ben-Dor G, Shapiro H (2006) Shock wave attenuation by grids and orifice plates. Shock Waves 16(41):1–15
5. Chan PC, Klein HH (1994) Study of blast effects inside an enclosure. J Fluids Eng Trans 116(3):450–455
6. Dadone A, Pandolfi M, Tamanini F (1971) Shock waves propagating in a straight duct with aside branch. In: Proceedings of the 8th International Shock Tube Symposium. London, UK, pp 1–13
7. Gu YC, Shi YY, Jin JL (2009) Engineering blasting safety. Press of University of Science and Technology of China, Hefei

8. Igra O, Wang L, Falcovitz J, Heilig W (1998) Shock wave propagation in a branched duct. Shock Waves 8(6):375–381
9. Janovsky B, Selesovsky P, Horkel J, Vejsa L (2006) Vented confined explosions in Stramberk experimental mine and AutoReaGas simulation. J Loss Prevent Proc 19(2–3):280–287
10. LSTC (2003) LS-DYNA Keyword User's Manual. Livermore Software Technology Corporation, California
11. Luccioni B, Ambrosini D, Danesi R (2006) Blast load assessment using hydrocodes. Eng Struc 28(12):1736–1744
12. Ohtomo F, Ohtani K, Takayama K (2005) Attenuation of shock waves propagating over arrayed baffle plates. Shock Waves 14(5):379–390
13. Pang L, Gao JC, Ma QJ, Chen JC, Meng QQ, Tan JL, Zhang Q (2013) Influence of bend structure on high-temperature flow after gas explosion. Exp Therm Fluid Sci 49:201–205
14. Qin B (2008) Research on shock wave propagating characteristic and rules inside the complex underground tunnels. Beijing Institute of Technology, China. (PhD Thesis)
15. Rigas F, Sklavounos S (2005) Experimentally validated 3-D simulation of shock waves generated by dense explosives in confined complex geometries. J Hazard Mater 121(1):23–30
16. Savenk CK (1979) Air shock wave in tunnel under mine, Translated by Long WQ, Metal Industry Press, Beijing
17. Smith PD, Mays GC, Rose TA, Teo KG, Roberts BJ (1992) Small scale models of complex geometry for blast overpressure assessment. Int J Impact Eng 12(3):345–360
18. Sugiyama Y, Homae T, Wakabayashi K, Matsumura T, Nakayama Y (2014) Numerical simulations on the attenuation effect of a barrier material on a blast wave. J Loss Prevent Proc 32:135–143
19. Wang C, Han WH, Ning JG, Yang YY (2012) High resolution numerical simulation of methane explosion in bend ducts. Safety Sci 50(4):709–717
20. Wang GH, Wang YX, Lu WB, Zhou W, Chen M, Yan P (2016) On the determination of the mesh size for numerical simulations of shock wave propagation in near field underwater explosion. Appl Ocean Res 59:1–9
21. Zhang Q, Qin B, Lin DC (2010) Estimation of pressure distribution for shock wave through the bend of bend laneway. Safety Sci 48(10):1263–1268
22. Zhang Q, Qin B, Lin DC (2013) Estimation of pressure distribution for shock wave through the junction of branch gallery. Safety Sci 57:214–222
23. Zhao HJ, Qian XM, Li J (2012) Simulation analysis on structure safety of coal mine mobile refuge chamber under explosion load. Safety Sci 50(4):674–678

Figures

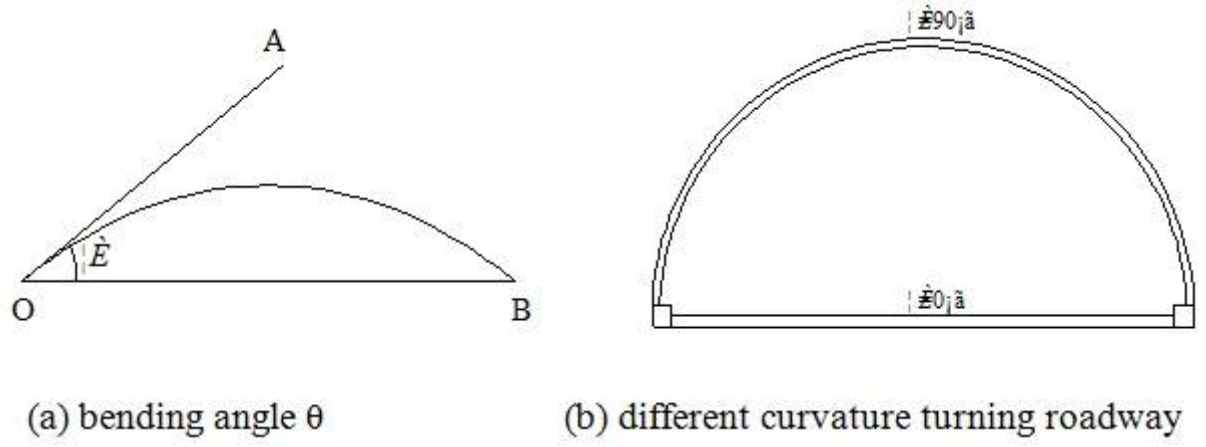

Figure 1

The bending angle and different curvature turning roadway

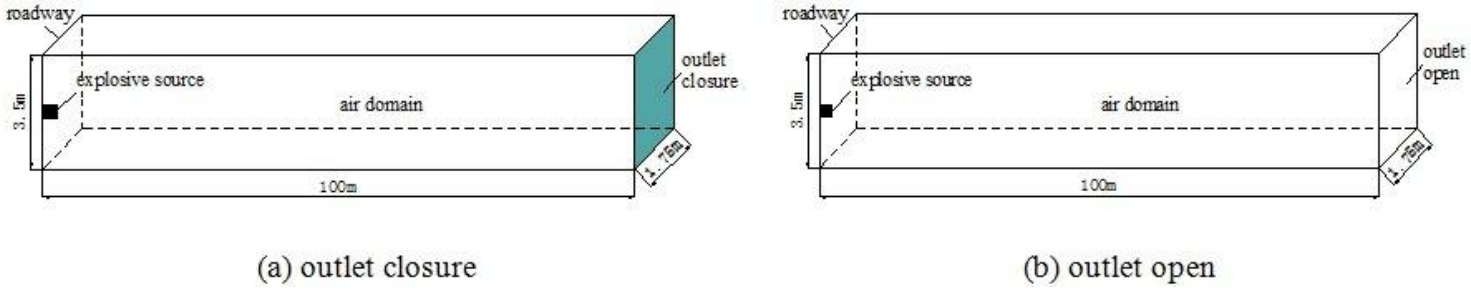

Figure 2

Explosion analysis model of roadway with θ=0°

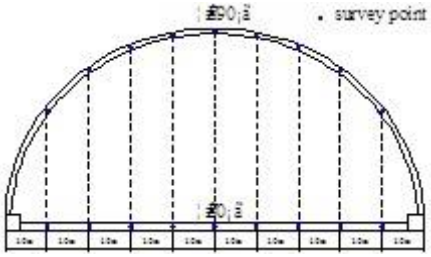

Figure 3

Survey point distribution in different curvature turning roadway

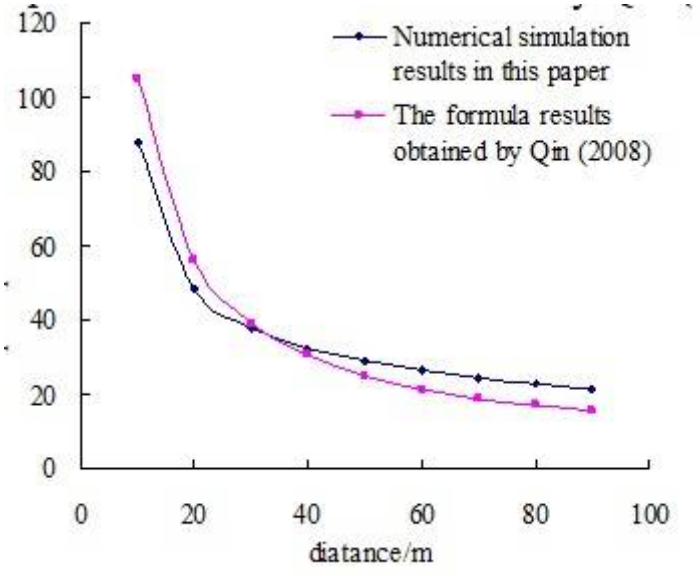

Figure 4

Comparison curves of peak pressure in roadway with θ=0° under the condition of outet open

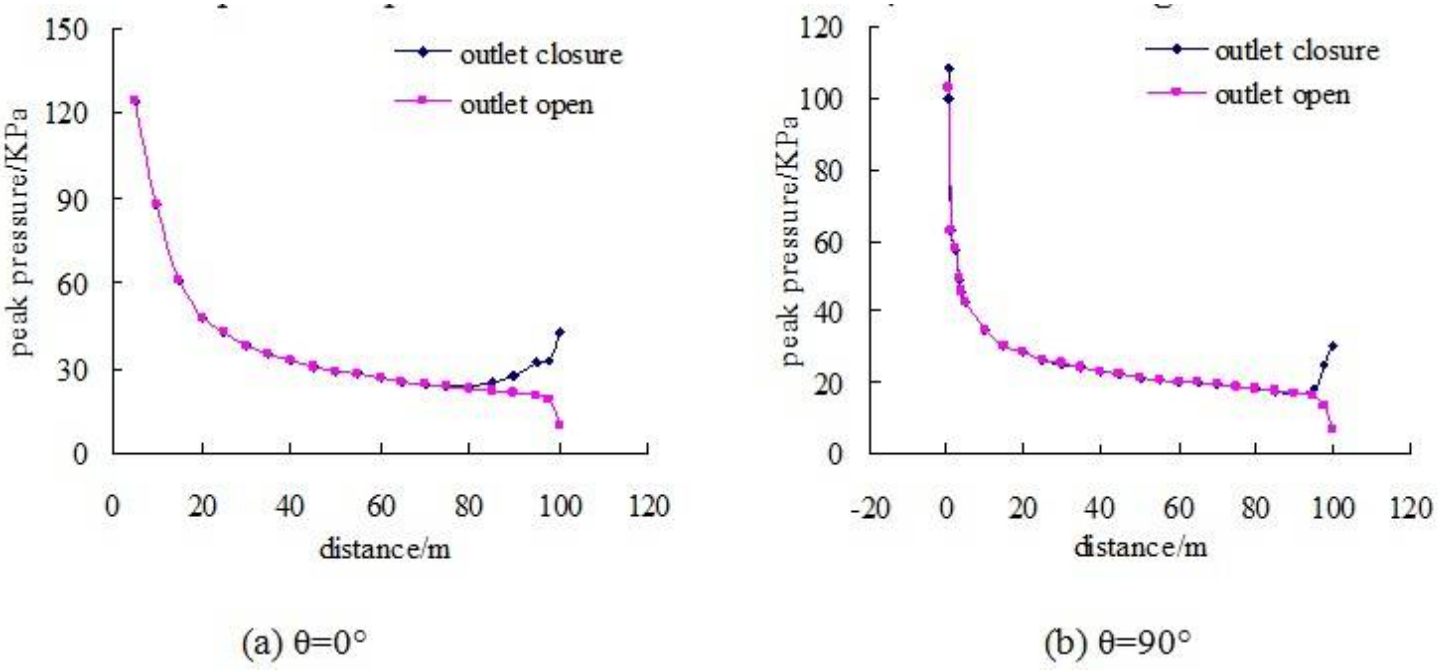

Figure 5

Peak pressure distribution in different curvature turning roadway

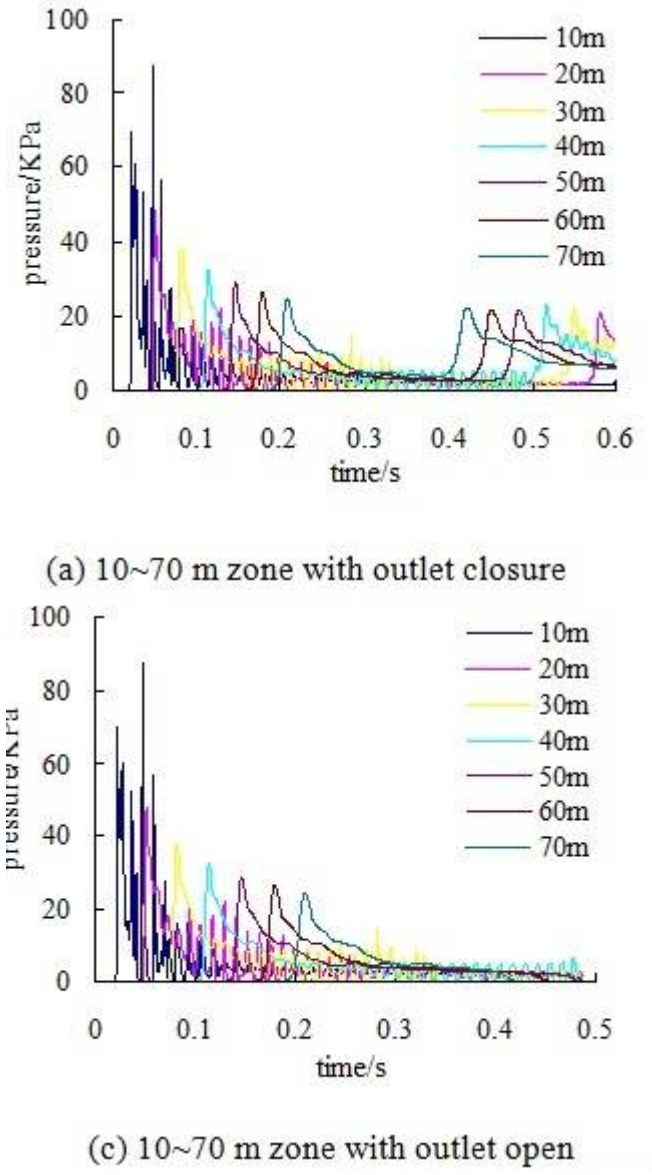

(a) 10~70 m zone with outlet closure

(b) 80~100 m zone with outlet closure

(c) 10~70 m zone with outlet open

(d) 80~100 m zone with outlet open

Figure 6

Pressure distribution in roadway with θ=0°

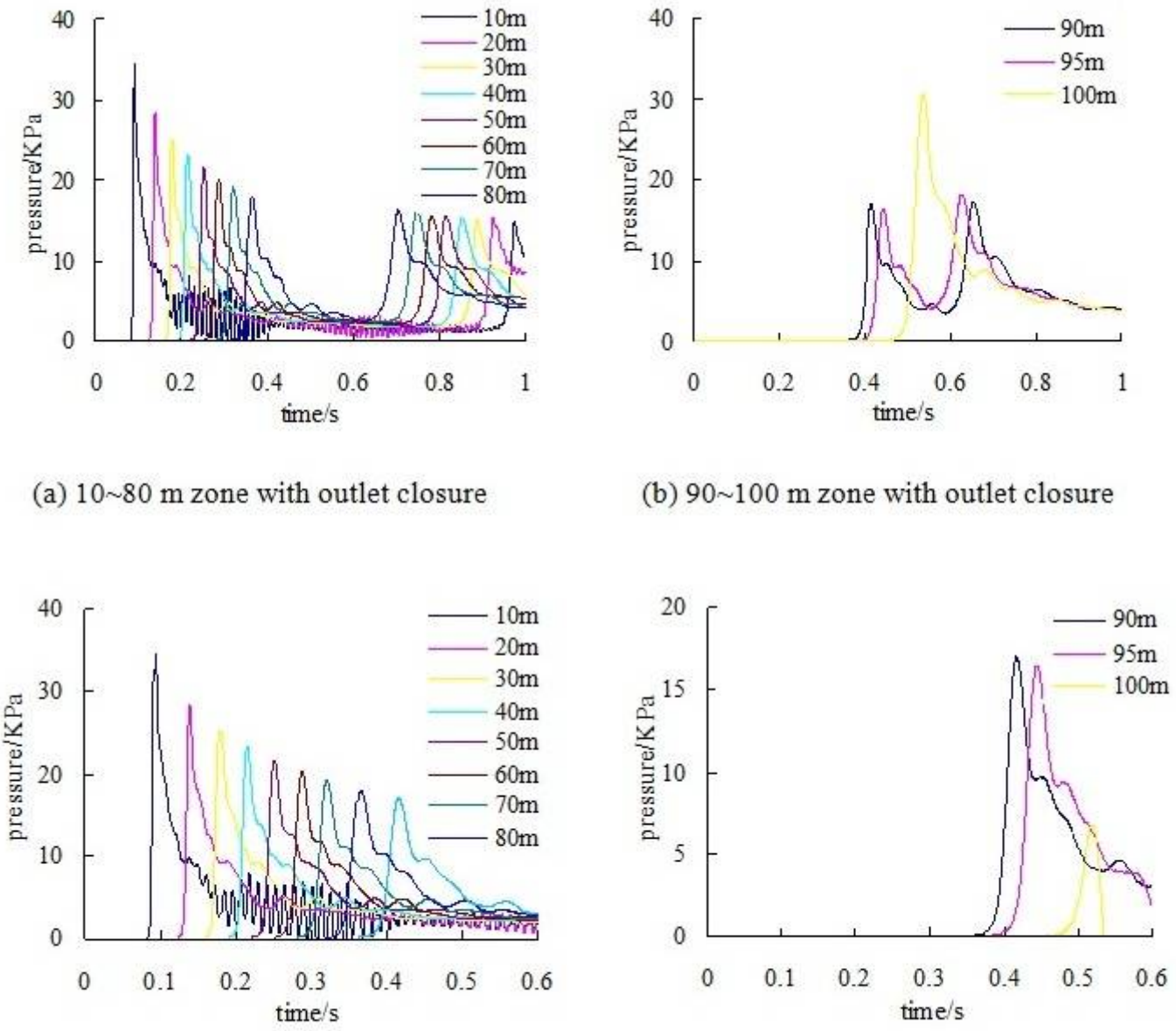

Figure 7

Pressure distribution in roadway with θ=90°

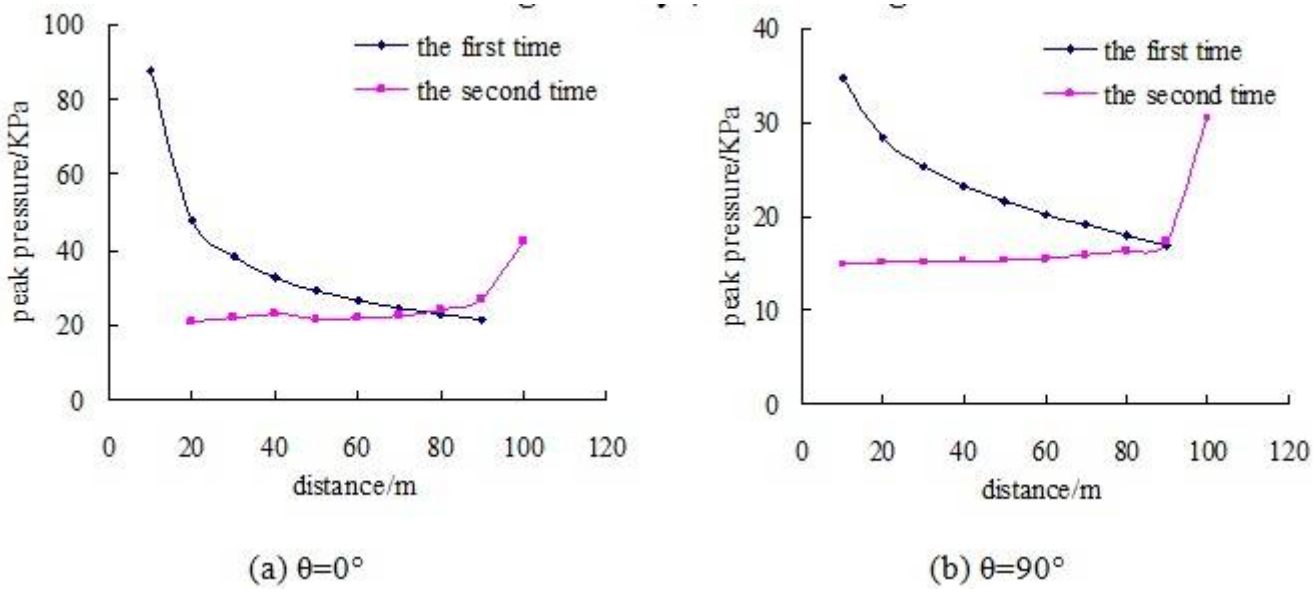

Figure 8

Peak pressure distribution in roadway of different curvature turning roadway with outlet closure

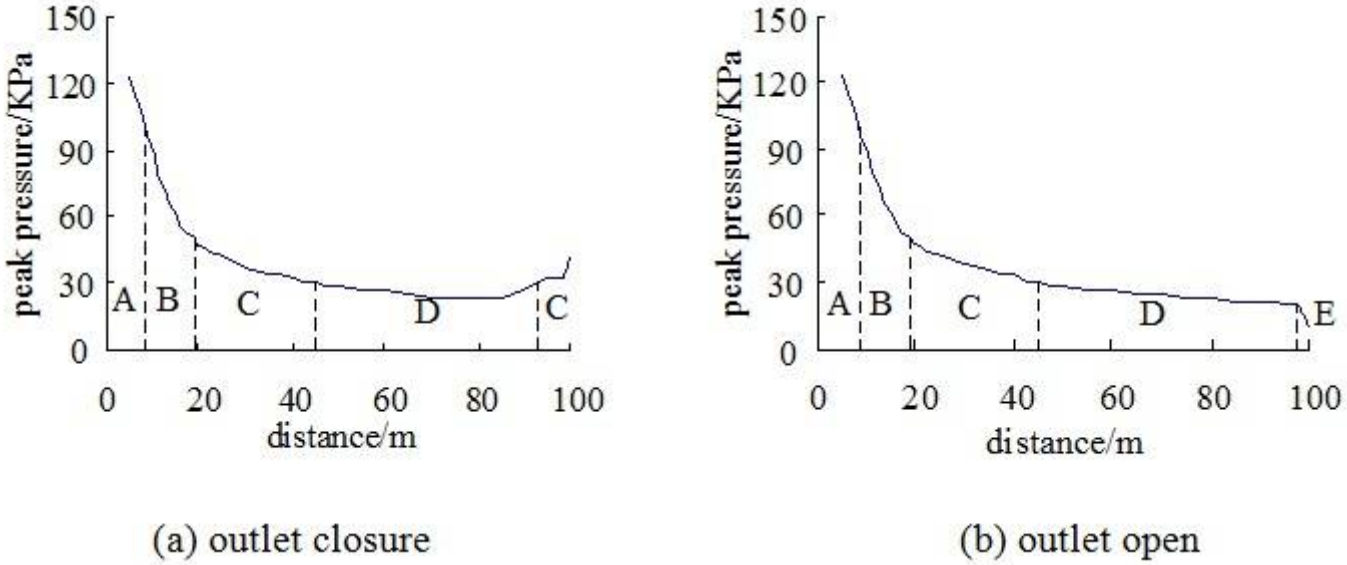

Figure 9

Explosive destruction effect partition in roadway with θ=0°

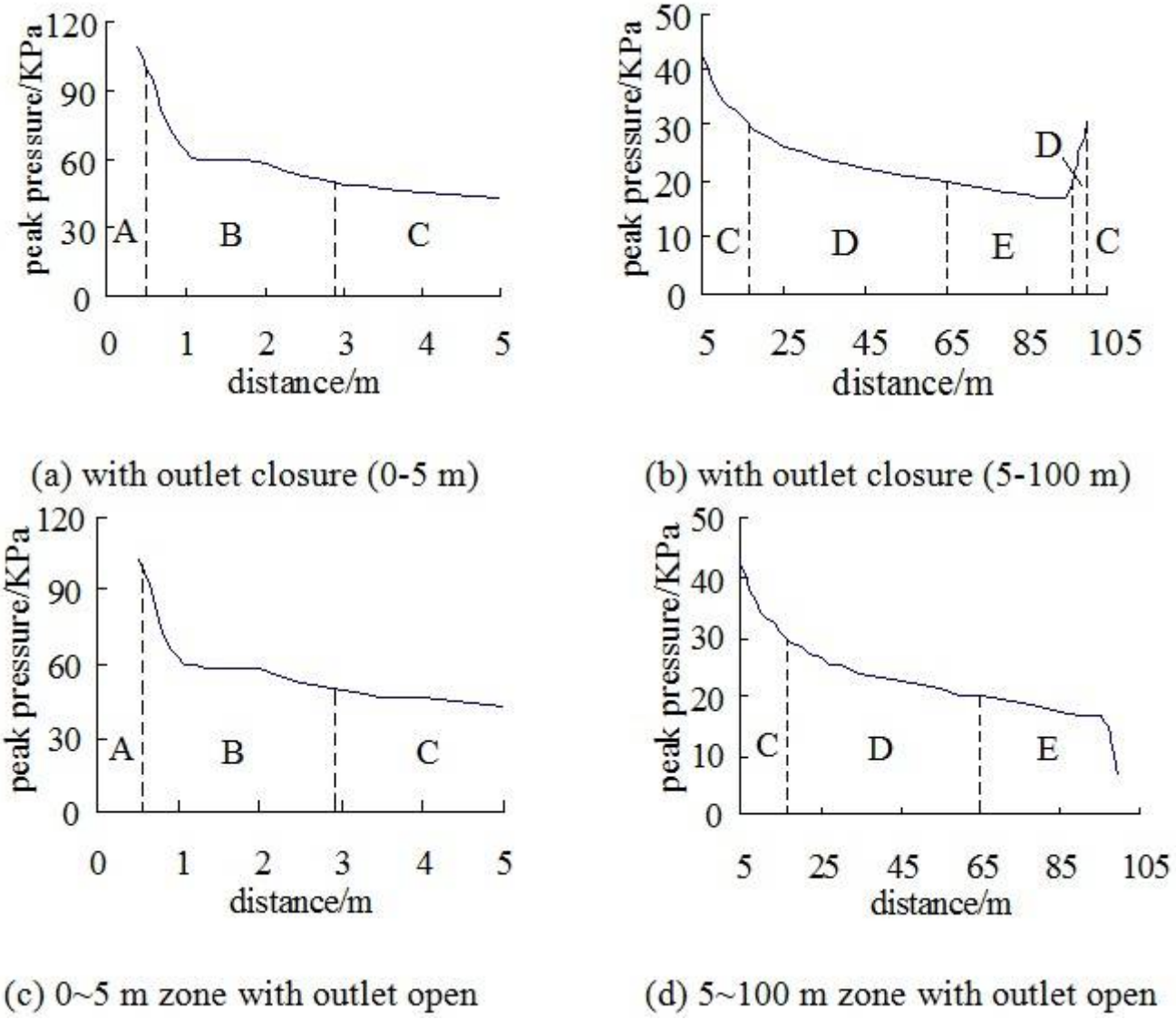

Figure 10

Explosive destruction effect partition in roadway with θ=90°